



Trade Science Inc.

Nano Science and Nano Technology

An Indian Journal

Full Paper

NSNTAIJ, 6(2), 2012 [73-78]

Structural and optical properties of nano thermal evaporated CuInS₂ films based solar cell

M.Dongol, M.Mobarak, A.El-denglawey*

Nano & Thin film Lab., Physics Department, Faculty of Science, South Valley University, Qena, (EGYPT)

E-mail: denglawey@lycos.com

Received: 1st February, 2012 ; Accepted: 28th February, 2012

ABSTRACT

Copper Indium disulfide, CuInS₂ or CIS films were prepared by thermal evaporation technique. Product films were prepared on glass substrates and heat-treated at various temperatures at fixed time. Structural and optical properties were investigated by using energy dispersive spectroscopy (EDS), X-Ray diffraction (XRD), Scanning electron microscope (SEM) and optical reflection and transmission measurements. The optical band gap increases within range 1.47 eV for the as prepared films to 1.61 eV for the annealed one. The annealing was performed within temperature range 523 up to 723 K. The increasing of the optical gap was attributed to both nano structure property and the enhancements of grain size. The obtained results were discussed in the light of current theoretical ideas.

© 2012 Trade Science Inc. - INDIA

KEYWORDS

CuInS₂;
CIS;
Transport properties;
EDS;
XRD;
Alloys;
Solar cell.

INTRODUCTION

The chalcopyrite semiconductors received considerable attention for their different promising practical applications namely, non-linear optics, light emitting diodes, photovoltaic optical detectors and solar cells^[1-7]. In between chalcopyrite semiconductors, the ternary CIS attracted an interest as a candidate for photovoltaic materials due to its optimum band gap of 1.5 eV^[8,9].

A large number of studies were devoted to CIS films. Owing to the difficulty to grow large single crystals of this compound, its fundamental properties are not well-understood^[10,11]. CIS-based solar cells reached efficiencies of almost 16% on an area of 1 cm²^[12]. However, little is known about the electronic properties of these cells. Since CIS does not include a toxic elements,

i.e. Se compared with Cu(In,Ga)Se₂, CIS is more environment-friendly than the selenium-contained material. Furthermore, the band gap of CIS is the most suitable for solar cell applications. In addition, there is no need to add other elements (e.g. Ga) to optimize the band gap also composition control of ternary material is much easier than that of quaternary ones^[13]. CIS thin films are fabricated by various methods, such as thermal evaporation^[14], molecular beam deposition^[9], ion plating^[15], chemical vapour deposition^[16,17], spray pyrolysis^[18-20] chemical bath deposition^[21], ion layer gas reaction (ILGAR)^[22] and electro-deposition^[23]. Among those available techniques, thermal evaporation was used. The present study tried to prepare CIS with better film quality as a solar cell, it also focused on the influence of thermal annealing on structural, stoichiometric, topographi-

Full Paper

cal and the optical properties of CIS films.

EXPERIMENTAL

Bulk material of chalcopyrite compounds CIS was prepared from highly pure Cu (5-nines purity), In (6-nines purity) and S (6-nines purity). Constituents were loaded into a fused silica tube with inner vacuum 10^{-6} Torr. Alloying of the elements was accomplished by putting the sealed tubes in a furnace with a rocking mechanism. The rocked motion was used to ensure the complete mixing of the materials. Furnace temperature program was adjusted firstly at $25^\circ\text{C}/\text{h}$ until 1050°C then keep constant for 60 hrs, and then silica tube was cooled in ice water. The result ingot was used as a source material to prepare CIS films. Thin films were prepared from the resultant by the thermal evaporation onto cleaned glass substrate using an Edward coating unit model E 306A, under a vacuum of 10^{-6} Torr. The deposition parameters were kept constant so a comparison of the results could be made under identical conditions. The film thickness, d was controlled at $1.6\ \mu\text{m}$ using a quartz crystal monitor. X-ray diffraction technique (XRD) was used to investigate the structure of the as prepared and annealed films using Philips diffractometer (type 1710) with Cu anode. To investigate the optical properties of CIS films, both transmittance, T and reflectance, R patterns of the amorphous films were measured at normal incidence at room temperature. A computerized SHIMADZU UV-1100 double beam spectrophotometer with 10 nm steps was used to measure both T and R within wavelength range (200–1100 nm). The tolerance of the film thickness is $\pm 1\%$ and in T and R is $\pm 1\%$. SEM analysis of CIS sample was performed using JEOL-JSM-5500LV scanning electron microscope operating at 10 kV.

RESULTS AND DISCUSSION

Structure analysis

EDS analysis

The stoichiometric ratio of copper and indium could be controlled from the starting composition of the precursor. Elemental analysis of the as prepared films was carried out at five different locations. Film composition

was studied by X-ray microanalysis revealing the presence of copper, indium and sulfur elements into the films. EDS was used to evaluate chemical composition of the film. The uncertainty of the present measurements is about 1% and EDS results indicated that the weight percentage of Cu, In and S was 26.20%, 47.35% and 26.45% respectively, which confirm that CIS is stoichiometric compound as depicted in Figure 1.

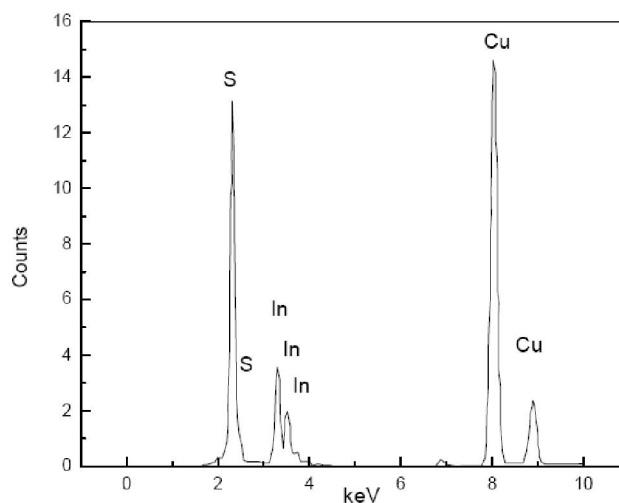


Figure 1 : EDS distribution of the constituent of the elements for as-deposited CuInS_2 .

XRD

Figure 2 (a), (b), (c) and (d) shows XRD profiles of the as prepared and annealed CIS films under vacuum 10^{-3} Torr which annealed at 523, 623 and 723 K for 1h. XRD peaks are matching with the standard ASTM data indicating the stoichiometry in the CIS. Due to annealing temperature, the CIS film undergoes crystalline transformations. No XRD peaks corresponding to any phase of

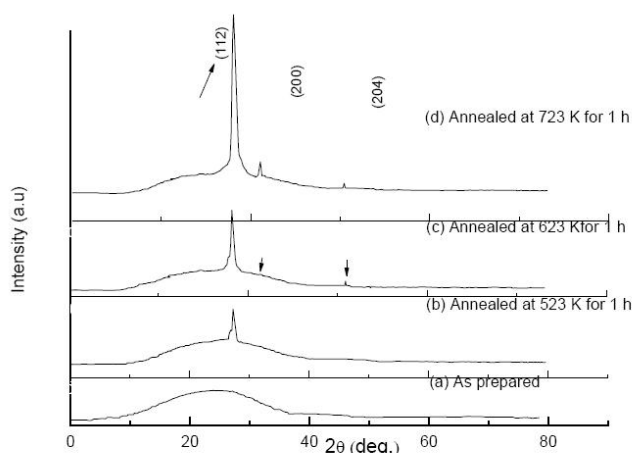


Figure 2 : XRD spectra for CuInS_2 films annealed at various annealing temperatures for 1 h.

crystalline CIS were observed for the as-prepared film as depicted in Figure 2(a), where the pattern shows a weak and broad reflections, indicating poor crystallinity of the films which confirm the amorphous structure. Improvement in the crystallinity of CIS films could be observed due to the increasing of annealing temperature that confirms the polycrystalline nature with (112), (200) and (204) preferred orientation, the main peak is (112).

The improvement of the crystallinity is supported by increasing of peaks intensity. Crystallite size could be calculated using Scherrer equation:

$$L = \lambda K / \beta \cos\theta \quad (1)$$

L is the mean crystallite dimension, K is constant (typically assumed 1), β is the peak FWHM in radians of 2θ and λ was taken as 1.54049 Å.

Values of crystallite size shows film nano structure property. Values of crystallite dimensions are 91, 104 and 110 nm for 523, 623, 723 K respectively which confirm the improvement of the CIS crystallinity, it is close to that obtained elsewhere^[24].

SEM

Film thickness was identified by cross section SEM micrograph, see Figures 3(a), 3(b), 3(c), 3(d) and 3(e) shows SEM images of the as prepared and annealed films at 523, 623 and 723 K respectively. Isolated particle growth with large grains is observed at the surface in particular at higher annealing temperatures surrounded by boundaries of smaller grains. The particle size was calculated. It was in the range of that obtained by XRD, which confirm nano structure property of CIS films. Particles were distributed homogeneously on the annealed surface, different numbers of particles with different size were observed as annealing temperature increases except the as prepared film; no particles could be identified due to amorphous state. These particles correspond to CIS phases, which would explain the XRD results. The particle size range is 91 nm to 110 nm. This features formed during nucleation and growth processes due to annealing effect. Surface of the as-deposited film looks dark gray, implying that the surface of the samples is free of Cu_xS second phase which confirmed by XRD patterns^[25], see Figure 2 and Figure 4. It is evident that there is an improvement of both crystallinity and uniformity of CIS film with increasing T_a . New features in Figure 3(e) could be identified and

attributed to growing of new (204) orientation CIS phase. The observed thickness of the CIS films from Figure 3(a) is about 1.6 μm which confirm the controlled experimental value. In addition, the glass substrate surfaces were well covered^[24].

Optical properties

Optical absorption coefficient was evaluated using transmittance, T and reflectance, R data according to^[27,28].

$$\alpha = \frac{1}{d} \ln \left[\frac{(1-R)^2}{T} \right] \quad (2)$$

d is the film thickness, R and T are the reflection and transmission respectively. To obtain an absorber material with high efficiency; photovoltaic applications need large absorption coefficient^[28]. The as prepared and annealed samples have higher absorption coefficient (10^4 – 10^6 cm^{-1}) in the visible spectral range. High absorption coefficient was supported by the dark gray color of the film as depicted in Figure 4. This result is very important due to that the spectral dependence of absorption coefficient affects the solar cells conversion efficiency. So according to^[28], CIS is a good candidate for photovoltaic applications. Absorption coefficient (α) is related to the incident photon energy (hv) by^[29]:

$$\alpha hv = B(hv - E_g)^m \quad (3)$$

B is a constant, h is the Planck constant, v is the frequency of the incident photon, E_g is the optical band gap, m is the index indicating the type of the transition. Values of m for allowed direct, allowed indirect, forbidden direct and forbidden indirect transitions are 1/2, 2, 3/2 and 3, respectively.

CIS is a well known direct band gap material, so putting $m = 1/2$, Eq. (3) can be written as

$$(\alpha hv)^2 = B(hv - E_g) \quad (4)$$

where B is a constant and hv is photon energy. According to this expression, $(\alpha hv)^2$ depends on (hv) linearly and intersects the energy axis at E_g . Figure 5 shows $(\alpha hv)^2$ versus photon energy (hv) for the as prepared and annealed CIS films.

Direct optical gaps were estimated and illustrated in Figure 6, this values agree to that obtained by^[30-32]. Generally, direct optical gap increases from 1.47 for as prepared to 1.61 eV with the increasing of annealing temperature.

Full Paper

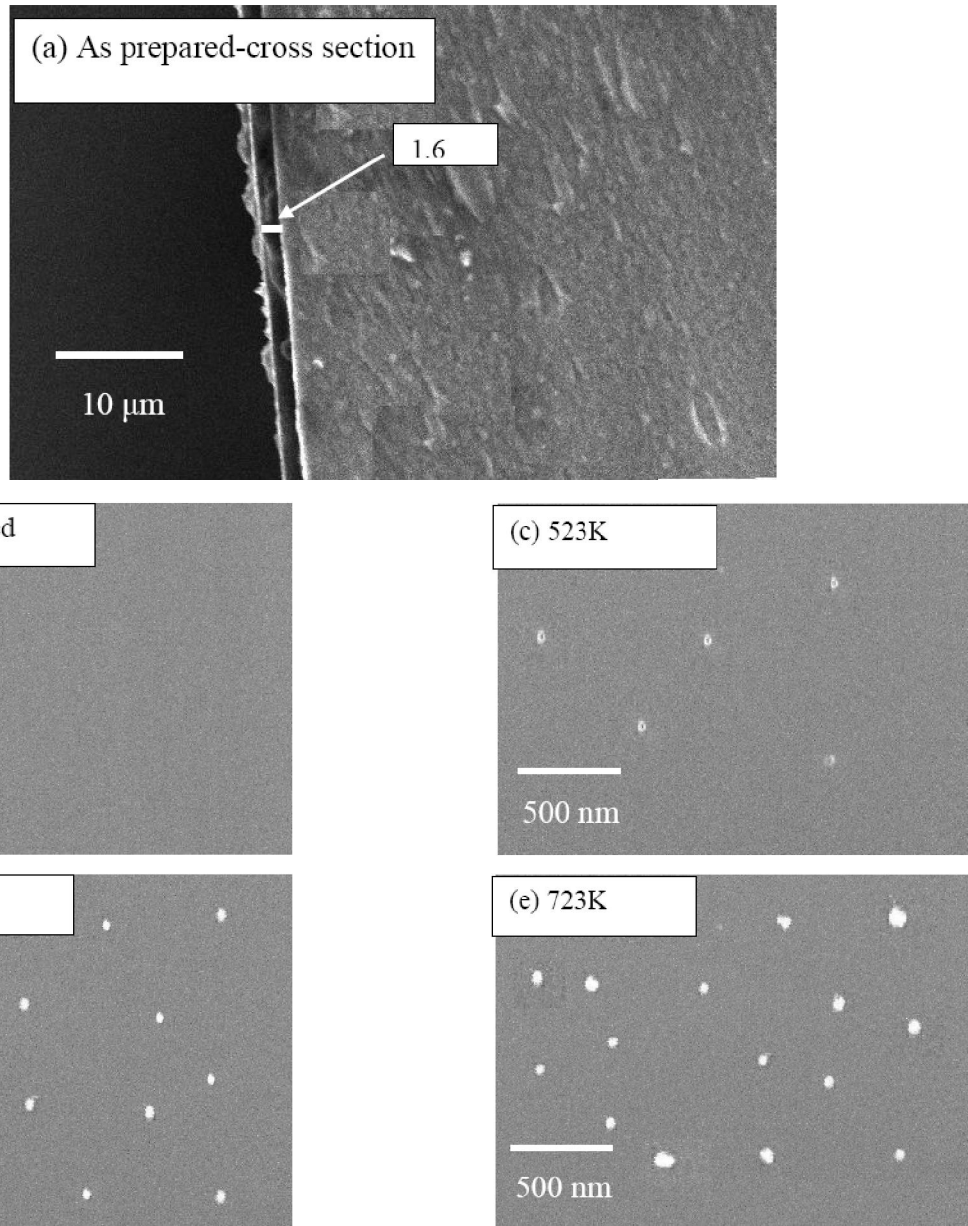


Figure 3 : SEM images for as prepared and annealed films.

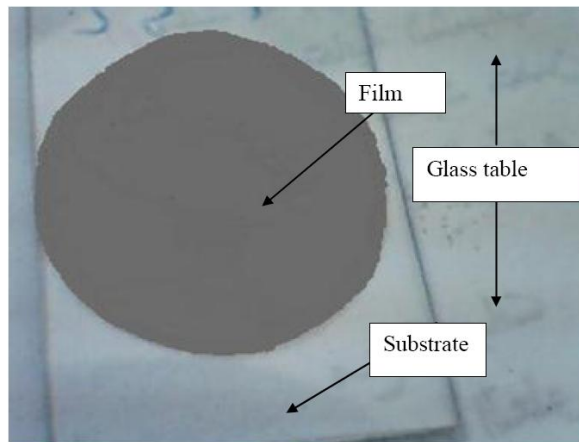


Figure 4 : Dark gray color of the as prepared CIS film.

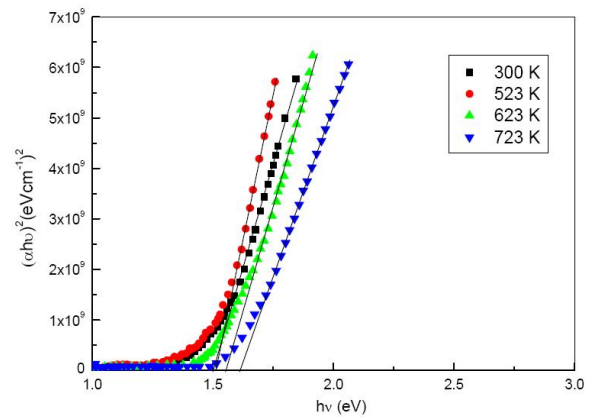


Figure 5 : $(\alpha hv)^2$ vs photon energy, (hv) for as prepared and annealed CuInS_2 films.

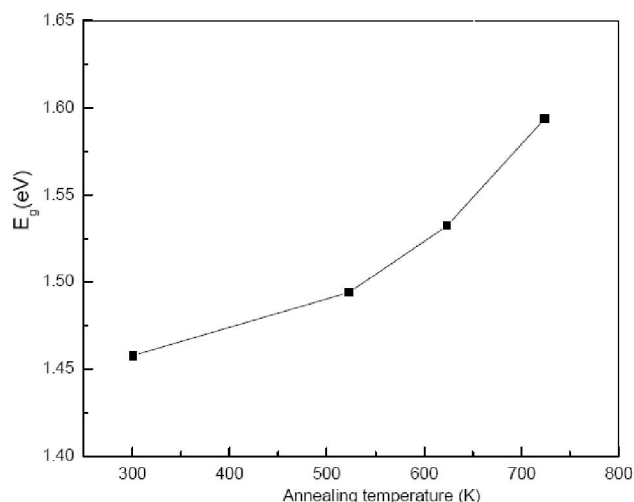


Figure 6 : E_g for as prepared and annealed CIS films

The obtained values of the optical gap of the as prepared CIS has a good agreement with that reported by other workers^[33-36]; and close to the optimum band gap value of CIS 1.5 eV^[8,9,20]. Direct optical gap value of powder CuInS_2 is 1.52 eV^[37]. Our values are lower than that reported in^[38]. Similar behavior of the optical gap as a function of annealing temperature was observed elsewhere^[25,30].

The increasing of E_g may be attributed to nano structure property, enhancement of grain size and the decrease of defects in nanostructure, which give rise to defect states and thus induce a smearing out of the absorption edge^[39-41]. Our obtained values were higher or lower, this was attributed to preparation methods, which are seriously affecting different properties.

CONCLUSION

Structural, morphological, and optical properties of the as prepared and annealed CIS films, prepared by thermal evaporation on glass substrates had been investigated. The stoichiometry of the product could be controlled and confirmed by EDS. There was a good agreement between the results of XRD, SEM and optical properties at different annealing temperatures. Results showed that the as prepared films were amorphous. Annealed films was characterized by polycrystalline structure with (112), (200) and (204) preferred orientations due to annealing temperature. Grain size range was 91 to 110 nm, which included within nanometric scale. Values of the optical gap start at 1.47 eV for as prepared film then increases regularly with

the increasing of annealing temperature to be 1.61 eV. The increasing of the optical gap was attributed to nano structure property and the enhancements of grain size hence the decrease of defects. The enhancement of grain sizes was confirmed by XRD, and SEM micrographs.

ACKNOWLEDGEMENTS

The authors express their thanks to Dr. S. Harb Associated Prof. of Phys., physics dept., Fac. of Sci., South Valley Univ. for his valuable assistance.

REFERENCES

- [1] W.Calvet, Hans-Joachim Lewerenz, Christian Pettenkofer; *Thin Solid Films*, **431-432**, 317 (2003).
- [2] S.Shirakata, Hideto Miyake; *J.Phys.Chem.Solids*, **64**, 2021 (2003).
- [3] T.Yamamoto, T.Watanabe, Y.Hamashoji; *Physica B: Condensed Matter*, **308-310**, 1007 (2001).
- [4] T.Watanabe, T.Yamamoto; *Jpn.J.Appl.Phys.*, **39**, L1280 (2000).
- [5] D.Cybulski, A.Opanowicz; *Crystal Research and Technology*, **32**, 813 (1997).
- [6] M.Quinetto, C.Rincon, R.Tovar, J.C.Woolley; *J.Phys.Condens Matter*, **4**, 1281 (1992).
- [7] J.Gonzalez, C.Rincon; *J.Phys.Chem.Solids*, **5**, 1093 (1990).
- [8] P.Guha, S.Gorai, D.Ganguli, S.Chaudhuri; *Materials Letters*, **57**, 1786 (2003).
- [9] Hirki Mastushita, Tomohiro Mihira, Takeo Takizawa; *J.Crystal Growth*, **197**, 169 (1999).
- [10] K.Wakita, K.Nishi, Y.Ohta, G.Hu; *J.Phys.Chem.Solids*, **64**, 1973 (2003).
- [11] K.Siemer, J.Klaer, I.Luck, D.Bruaunig; *Thin Solid Films*, **387**, 222 (2001).
- [12] H.W.Schock; in: *Proceedings of the 12th European Photovoltaic Solar Energy Conference*, 944 (1994).
- [13] S.Y.Lee, B.O.Park; *Thin Solid Films*, **516**, 3862 (2008).
- [14] S.Bandyopadhyaya, S.Chaudhuri, A.K.Pal; *Sol.Energy Mater.Sol.Cells*, **60**, 323 (2000).
- [15] M.Gossila, H.Metzner, J.Conrad, U.Geyer, T.Hahn; *Thin Solid Films*, **268**, 39 (1995).
- [16] K.I.Kondo, H.Sano, S.Nakamura, K.Sato, H.Hirasawa; *Sol.Energy Mater.Sol.Cells*, **49**, 327 (1997).
- [17] J.A.Hollingsworth, K.K.Banger, M.H.-C.Jin,

Full Paper

- J.D.Harris, J.E.Cowen, E.W.Bohannon, J.A.Switzer; Thin Solid Films, **431-432**, 63 (2003).
- [18] A.N.Tiwari, D.K.Pandya, K.L.Chopra; Thin Solid Films, **130**, 217 (1985).
- [19] M.Krunks, V.Mikli, O.Bijakina, H.Rebane, A.Mere, T.Varema, E.Mellikov; Thin Solid Films, **361-362**, 61 (2000).
- [20] A.Katerski, M.Danilson, A.Mere, M.Krunks; Energy Procedia, **2**, 103 (2010).
- [21] S.Mahmoud, A.H.Eid; Fizika A, **4**, 171 (1997).
- [22] S.Lindroos, A.Arnold, M.Leskela; Appl.Surf.Sci., **158**, 75 (2000).
- [23] S.Kuranouchi, T.Nakazawa; Sol.Energy Mater.Sol.Cells, **50**, 31 (1998).
- [24] J.Qiu, Z.Jin, J.Qian, Y.Shi, W.Wu; J.Cryst.Growth, **282**, 421 (2005).
- [25] X.P.Liu, L.-X.Shao; Surface & Coatings Technology, **201**, 5340 (2007).
- [26] D.E.Milovzorov, A.M.Ali, T.Inokuma, Y.Kurata, T.Suzuki, S.Hasegawa; Thin Solid Films, **382**, 47 (2001).
- [27] T.M.Wang, S.K.Zheng, W.C.Hao, C.Wang; Surf.Coat.Technol., **155**, 141 (2002).
- [28] V.V.Kindyak, V.F.Gremenonok, I.V.Bodnar, V.Rud Yu, G.A.Madvedkin; Thin Solid Films, **250**, 33 (1994).
- [29] N.F.Mott, E.A.Davis; Electronic Processes in Non-Crystalline Materials, Clarendon Press, Oxford, (1971).
- [30] M.Ben Rabeh, M.Kanzari, B.Rezig; Thin Solid Films, **515**, 5943 (2007).
- [31] K.Das, S.K.Panda, S.Gorai, P.Mishra, S.Chaudhuri; Materials Research Bulletin, **43**, 2742 (2008).
- [32] M.Sahal, B.Mari, M.Mollar; Thin Solid Films, **517**, 2202 (2009).
- [33] M.Zribi, M.Kanzari, B.Rezig; Materials Letters, **60**, 98 (2006).
- [34] M.Ben Rabeh, M.Kanzari; Thin Solid Films, **519**, 7288 (2011).
- [35] J.G.Hernandez, P.M.Gorley, P.P.Horley, O.M.Vartsabyuk, Y.V.Vorobiev; Thin Solid Films, **403&404**, 471 (2002).
- [36] A.Bollero, J.F.Trigo, J.Herrero, M.T.Gutiérrez; Thin Solid Films, **517**, 2167 (2009).
- [37] J.Zhou, S.Li, X.Gong, Y.Yang, Y.Guo; Materials Letters, **65**, 2001 (2011).
- [38] C.Mahendran, N.Suriyanarayanan; Physica B, **405**, 2009 (2010).
- [39] J.L.Shay, J.H.Wernick; Ternary Chalcopyrite Semiconductors, Pergamon, Oxford, (1975).
- [40] L.Y.Sun, L.L.Kazmerski, A.H.Clark, P.J.Ireland, D.W.Morton; J.Vac.Technol., **15**, 265 (1978).
- [41] M.M.El-Nahass, M.Dongol, M.Abou-zied, A.El-Denglawey; Physica B, **368**, 179 (2005).